Supplementary Information

Micro elastofluidic liquid diode for programmable unidirectional flow control

Haotian Cha^a, Fariba Malekpour Galogahi^a, Quang Thang Trinh^a, Sharda Yadav^a, Jun Zhang^{a,b}, Hongjie An^c, Qin Li^b, Nam-Trung Nguyen^{*a},

- ^a Queensland Quantum and Advanced Technologies Research Institute, Griffith University, Nathan, Queensland 4111, Australia. E-mail: nam-trung.nguyen@griffith.edu.au
- ^{b.} School of Engineering and Built Environment, Griffith University, Nathan, Queensland 4111, Australia
- ^c School of Environment and Science, Griffith University, 170 Kessels Road, Queensland 4111, Australia

Table of contents

- **Fig. S1** Schematic illustration and optical microscope images of the fabrication process for the patterned structures on the PDMS substrate.
- Fig. S2. Investigation of surface cracking behaviour on PDMS substrates under y-axis stretching.
- **Supplementary Video S1.** Pinned flow condition in surface-patterned geometry.
- **Supplementary Video S2.** Unidirectional flow condition in surface-patterned geometry.
- Supplementary Video S3. Bidirectional flow condition in surface-patterned geometry.
- **Supplementary Video S4.** Unidirectional flow progression across a single unit in surface-patterned geometry.
- **Supplementary Video S5.** Pinned flow condition in open-channel geometry.
- **Supplementary Video S6.** Unidirectional flow condition in open-channel geometry.

Supplementary Video S7. Bidirectional flow condition in open-channel geometry.

Supplementary Video S8. Unidirectional flow progression across a single unit in open-channel geometry.

Supplementary Video S9. Reversible lateral migration of liquid under y-axis stretching.

Supplementary Video S10. Application in sweat-side transport within integration platform.

Fig. S1 Schematic illustration and optical microscope images of the fabrication process for the patterned structures on the PDMS substrate.

To fabricate the 2D patterned structures on PDMS, a localized masking method using double-sided tape (3M, 8000 series) was employed. First, chevron-ratchet patterns were precisely cut into the tape using a femtosecond laser cutting system (A Series, Oxford Lasers, UK). A thin PDMS layer (~500 µm thickness) was then prepared. After peeling off the protective liner, the laser-patterned tape was carefully laminated onto the PDMS surface. Subsequently, the assembly was treated with oxygen plasma using a plasma cleaner (PDC-002-CE, Harrick Plasma, USA). The treatment duration was varied according to the experimental design. After plasma exposure, the tape was gently removed to reveal the patterned regions. Care was taken to minimize substrate vibration during tape removal to preserve the fidelity and flatness of the patterns. The resulting structure exhibited hydrophilic patterned regions corresponding to the exposed PDMS, while the masked areas remained hydrophobic, thus achieving localized surface modification. It is important to minimize the delay between tape removal and fluid testing to prevent time-dependent variations in surface properties.

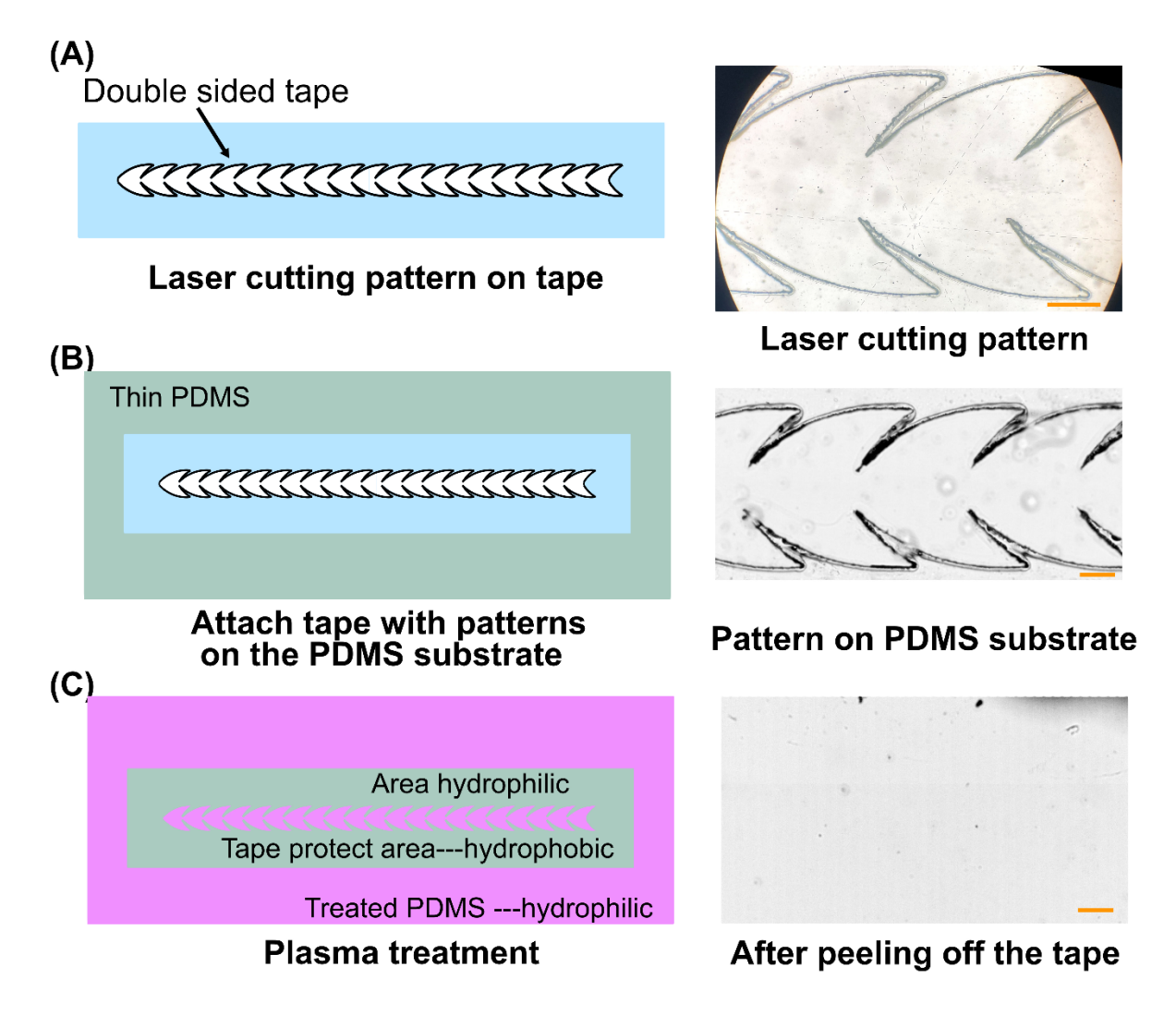


Fig.S1 Schematic illustrations (left) and corresponding optical microscope images (right) of the fabrication process for patterned structures on PDMS substrates. (A) Laser cutting of chevron-ratchet geometry patterns into a double-sided PET tape using a femtosecond laser system. The inset shows the resulting pattern features on the tape. (B) Laminating the patterned tape onto a thin PDMS substrate ($\sim 500~\mu m$ thickness). Optical micrographs show the transferred pattern on the PDMS surface prior to treatment. (C) Oxygen plasma treatment of the assembled substrates with varying exposure durations, followed by tape removal. The resulting surface exhibits an invisible boundary between hydrophilic (plasma-exposed) and hydrophobic (tape-protected) regions, forming localized wettability contrast. Scale bar: $100~\mu m$.

Fig. S2. Investigation of surface cracking behaviour on PDMS substrates under y-axis stretching.

An indirect approach was employed to assess surface cracking in PDMS during uniaxial elongation. A 500 nm-thick gold layer was uniformly sputtered onto the PDMS open-channel surface to visualize surface deformations. The substrate was then stretched along the y-axis using the custom mechanical platform, and crack formation was monitored via optical microscopy. As shown, increasing elongation distance induced more frequent and wider surface cracks. The cracks were oriented orthogonally to the stretching direction, indicating strain-localized surface rupture. This indirect method reflects changes in surface wettability during deformation: stretching exposes hydrophobic PDMS regions beneath the cracked PDMS surface, altering the local wetting behaviour. This change in surface energy may cause the liquid to migrate laterally, aggregating along the sidewall regions while leaving the central channel temporarily dry. Upon releasing the strain, the microcracks gradually closed, restoring the overall hydrophilicity and allowing the liquid to reoccupy the original channel area. This mechanism provides a plausible explanation for the reversible liquid migration phenomenon observed under y-axis stretching, Fig. 5 (F). Future work could focus on leveraging straininduced cracking to actively control liquid localization and transport in flexible microfluidic systems.

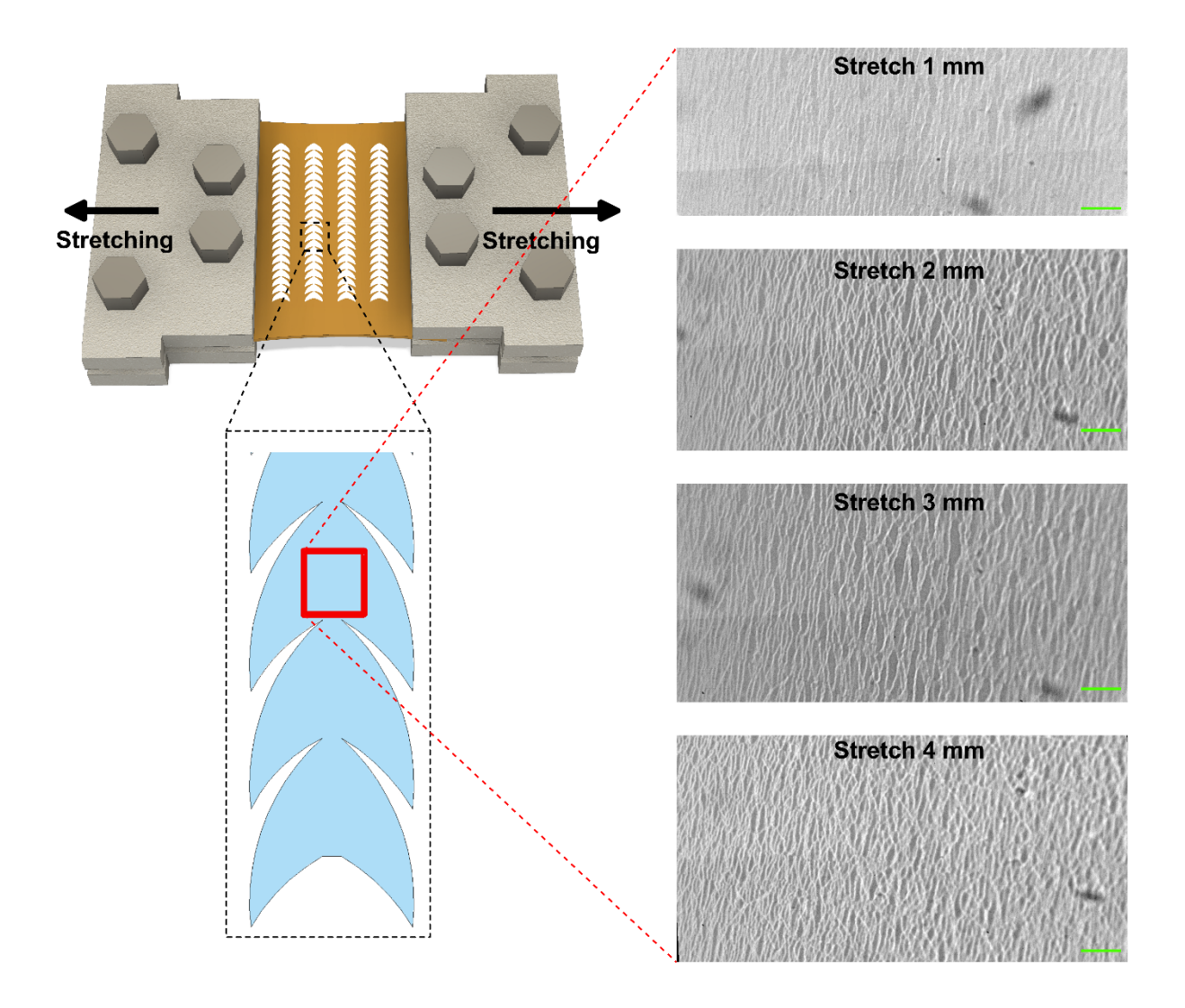


Fig. S2. Visualization of surface cracking on PDMS substrates under y-axis stretching. A \sim 500 nm-thick gold layer was sputter-deposited onto the PDMS surface to facilitate crack observation. The substrate was stretched along the y-axis using a custom mechanical platform while monitoring surface deformation via optical microscopy. As the elongation increased, wider and more pronounced cracks developed, oriented perpendicular to the stretching direction. Scale bar: 100 μ m.

Supplementary Video S1. Pinned flow condition in surface-patterned geometry.

Supplementary Video S2. Unidirectional flow condition in surface-patterned geometry.

Supplementary Video S3. Bidirectional flow condition in surface-patterned geometry.

Supplementary Video S4. Unidirectional flow progression across a single unit in surface-patterned geometry.

Supplementary Video S5. Pinned flow condition in open-channel geometry.

Supplementary Video S6. Unidirectional flow condition in open-channel geometry.

Supplementary Video S7. Bidirectional flow condition in open-channel geometry.

Supplementary Video S8. Unidirectional flow progression across a single unit in open-channel geometry.

Supplementary Video S9. Reversible lateral migration of liquid under y-axis stretching.

Supplementary Video S10. Application in sweat-side transport within integration platform.